Study of the CMS hadron outer calorimeter support to the level 1 muon trigger

Mitzi V. Urquiza González, Universidad Nacional Autónoma de México (UNAM), Mexico

Supervisor: Ashraf Mohamed, Deutsches Elektronen Synchrotron (DESY), Germany

September 5, 2018

Abstract

For the CMS muon detector, it was studied the possibility of the Outer Hadronic Calorimeter (HO) to work as a support for the level 1 muon trigger in the CMS Barrel region in case of failure of the first muon station (MB1). This study explores a way to include information from the HO into the Barrel Muon Track Finder (BMTF) algorithm to compensate the efficiency loss due to the failure of the MB1. It was found that for the muon track reconstructed from two stations including the MB1, the majority use the MB2. The BMTF efficiency drops by 15.38% due to the MB1 failure.This drop is due to the MB12, MB13 and MB14 track that are expected to be lost. HO can recover 75% of them. Finally, this study can be extended to include the analysis of the resolution of the transverse momentum for the MB3 and MB4 station using the HO as part go the muon system.

Contents

1 Introduction

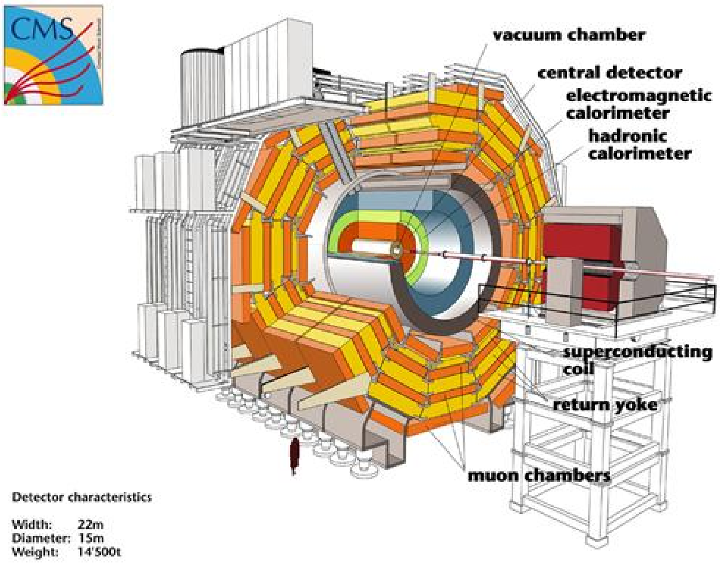

Figure 1: Left half of the model of CMS experiment at the LHC in CERN

The Compact Muon Solenoid (CMS) experiment illustrated in figure **??**, is one of the four experiments run at the LHC in Geneva, Switzerland. Its areas of study range from the study of the Standard Model, including the Higgs boson, to searching for the possible candidates that could make up dark matter. Even though it shares the same scientific goals as the ATLAS experiment, it differs in the technical solutions and a different magnet-system design[**?**].

The CMS detector uses a high resolution tracker in a 4 tesla solenoid magnet to measure the momentum of each charged particle, and uses the Hadronic Calorimeter (HCAL) and the Electromagnetic Calorimeter (ECAL) to measure the energy of each particle whether they are charged or neutral[**?**]. Due the geometrical structure of the CMS experiment, the coordinate system to know the localization of every component and interaction is as follows:
It is a cartesian coordinate system with the origin at the targeted interaction point or collision point inside the experiment, the $x - axis$ pointing inwards to the LHC center, the $y - axis$ vertically upwards and the $z - axis$ along the beam direction. As such, the ϕ is the azimuthal angle which is measured in the xy plane from the $x - axis$, the θ is the angle which is measured from the $z - axis$ and the r radial coordinate from the center on the xy plane.

Nevertheless, the angle θ is usually reformulated as a pseudo-rapidity η where η is

$$\eta = -log(tan(\frac{\theta}{2}))$$

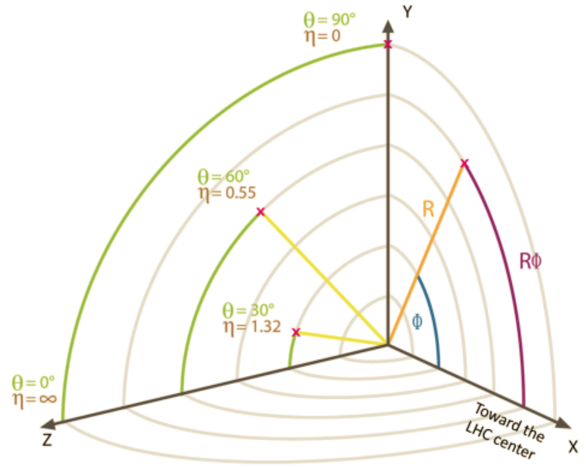

Figure 2: Sketch of the CMS coordinate system [?]

This defines the angle between a line and the beam axis in the XY plane; and that guarantees that the particle flux originating from hadron-hadron collisions is about the same for every η interval[?, ?]. Figure ?? sketches this coordinate system.

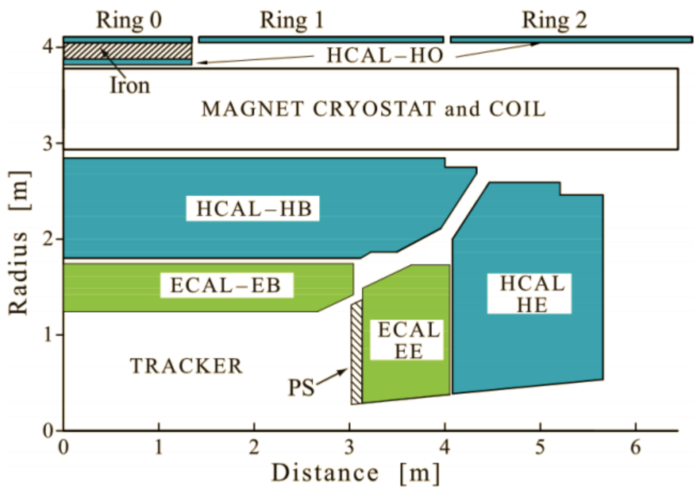

Figure 3: Locations of the HCAL and the Electromagnetic Calorimeters (EB, EE) in the CMS in the r-z plane[?, ?].

Given that this report is mainly about the hadron calorimeter and the muon system, the rest of the detectors that form the CMS experiment will be only shown in the figure ??. Figure ?? shows a diagram with the locations of the calorimeters that made the HCAL. The HCAL consists of a forward part (HF), an endcap part (HE) and an inner or barrel part (HB); being the HB and HE sampling calorimeters made of alternating layers of brass absorber and plastic scintillator[?, ?].

Figure ?? shows the barrel region (HB) is located inside the magnetic coil or the solenoid, followed by the HO; which supports the HB for high hadronic activity that may scape the detection on the previous calorimeters. The HO consists of a single layer of plastic scintillator except for the central region that has a double layer. The HO is mounted in iron return yoke[?]. In total, the HO is composed of 5 concentric rings or wheels.

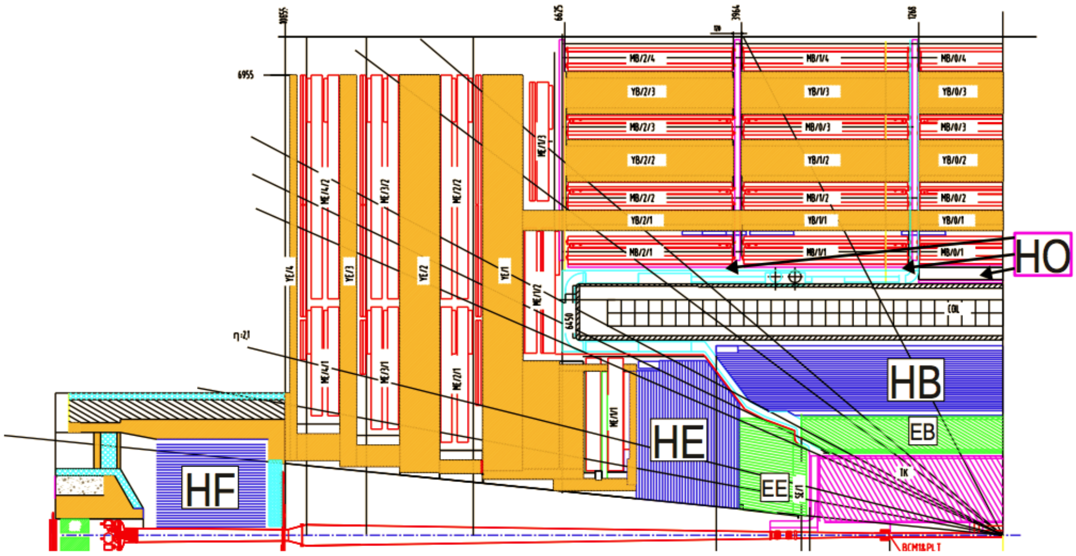

Figure 4: In orange, the location of the three components of the Muon System at CMS[?]

1.1 Muon detector

The outermost part of the CMS experiment. It is composed of magnet return yoke, equipped with gaseous detector chambers to identify the muons and to measure their momentum. The muon detector consists of 4 stations and each of them is also composed from 5 separated wheels[?]. Each barrel is then sectioned in 12 segments in the azimuthal angle.

The muon system has three types of gas detectors that are integrated for three parts: drift tubes (DT), cathode strip chambers (CSCs), and resistive plate chambers (RPCs). In total, there are 250 DT, 540 CSCs and 610 RPCs, with their corresponding positions shown in figure ??[?].

For the Run 2 in 2015 at the LHC, the HCAL made a series of upgrades, including new silicon photomultipliers to improve the performance of it. Since the BMTF algorithm requires to have at least two valid hits in two different muon stations to form a track, having a failure in the MB1 will cause a drop of the level 1 muon trigger efficiency. This paper studies how much the HO can compensate this inefficiency.

2 BMTF

In order to form a muon track, the BMTF combines information from different muon stations to from a trigger primitive, at the same time, the BMTF measures the bending angle between the different muon stations of each track to calculate the transverse momentum (pT)[?]. On the other hand, the TwinMux, a new hardware component in the level 1 muon trigger, combines the HO information with muon information so a muon track can be formed with the HO too.

For this study, only the muon tracks formed using information from only two station are taken into consideration, specifically those that are made with the MB1 and any other station. An algorithm was used to compare the same muon tracks that can be formed with the HO and if the HO has a coincidence with the muon track formed from the MB stations. This algorithm is explained in the next subsection.

2.1 Algorithm for HO-MB matching

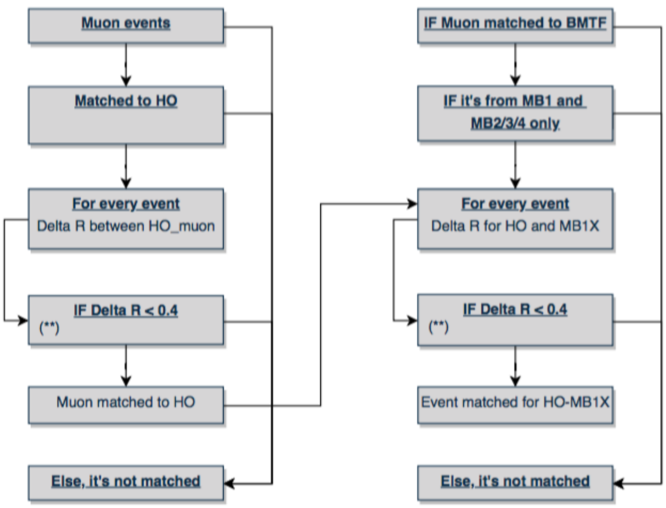

Figure 5: Basic overview of the matching algorithm for a muon event[?]

Figure ?? illustrates the algorithm used to find the MBTF track that can be matched to one of the HO hits. The algorithm uses primarily a geometrical condition using the

ϕ_{muon} and η_{muon} position of each event and subtracts it from the ϕ and η position using the muon information from the HO. This geometrical conditions gives a distance called $\Delta R = \sqrt{(\Delta\phi^2 + \Delta\eta^2)}$.

On the left of figure ??, the matching is done looping over every event and looking for a HO coincidence what the muon within the cone size of ΔR of 0.4, then the selection is made. This particular HO-muon like hits stored to prevent double matching.

On the left, the matching is done between the BMTF MB1X type track and the reconstructed muon with the same cone size of ΔR of 0.4, where the X represents the other muon station that was used, that is, X can be 2, 3 or 4. This gives a BMTF-muon like object which is then matched against the HO-muon like object from the first step again with the same cone size of ΔR of 0.4

After doing all these geometrical matches, the results and analysis are presented on the next section.

3 Analysis and results

Using SingleMuon_Run2017C-ZMu-PromptReco-v3_RAW-RECO data, the code with the algorithm explained in the last section was run to estimate how much the HO can recover from the lost tracks due to MB1 failure. Figure **??** shows the percentage of tracks that would be lost in the MB12 stations, as well the percentage of tracks for the MB13 and MB14 stations. Figures **??** also shows the percentage of tracks that the HO can recover in combination with the MB2 station, figure **??** for the HO and MB3 station, and figure **??** for the HO and MB4 station.

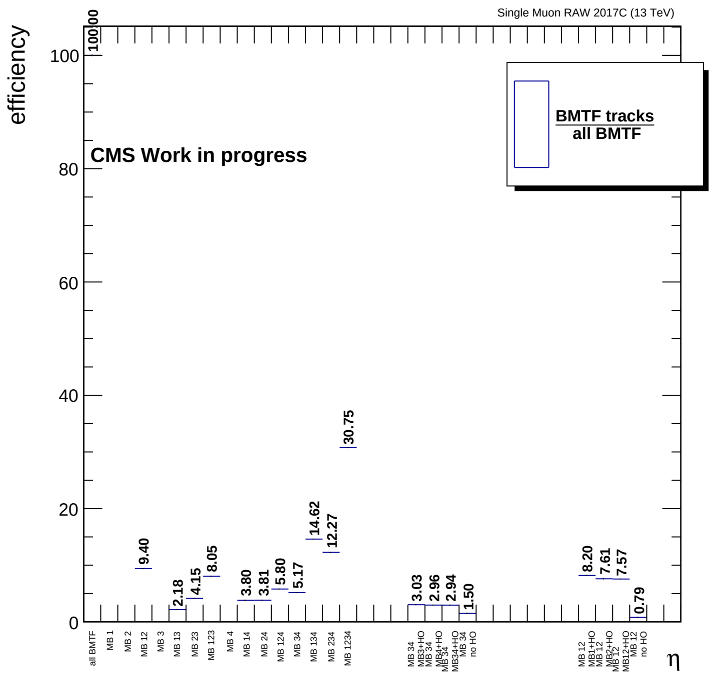

Figure 6: For MB12, number of each BMTF track type and HO composition for MB12

BMTF loss is estimated to be 9.40% only from the MB12 tracks in the case of MB1 failure and HO recovery is estimated to be 8.20%, that is 87% out of the 9.40%.

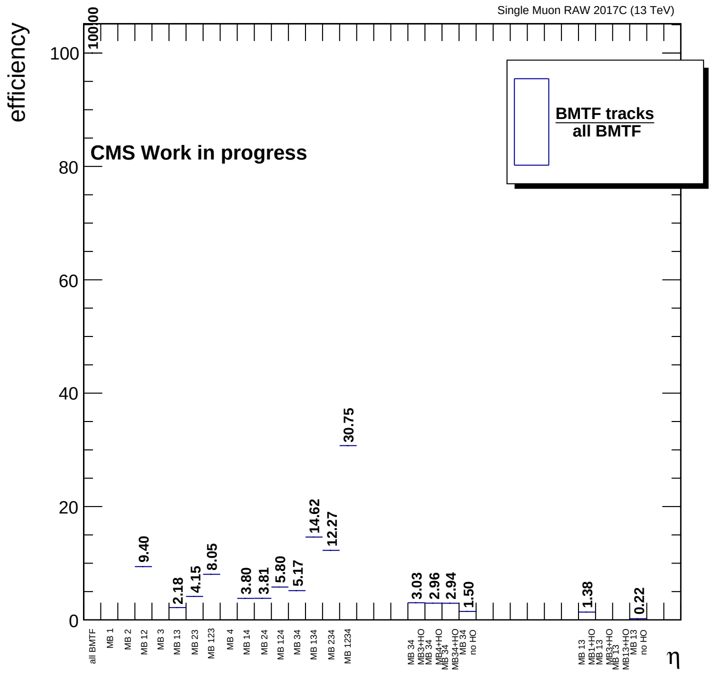

Figure 7: For MB13, number of each BMTF track type and HO composition for MB13

BMTF loss is estimated to be 2.18% from the MB13 tracks in the case of MB1 failure and HO recovery is estimated to be 1.38%. That is, a 63% recovery out of the 2.18%.

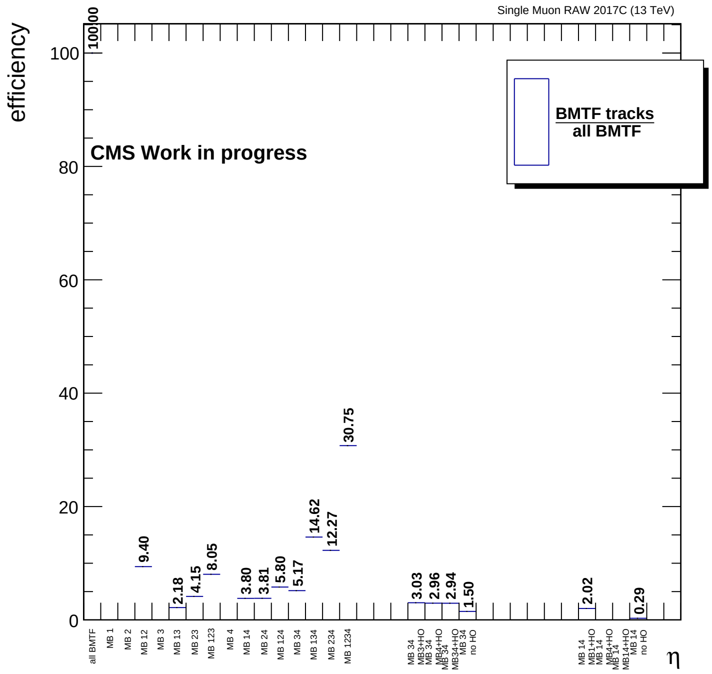

Figure 8: For MB14, number of each BMTF track type and HO composition for MB14

Finally, BMTF loss is estimated to be 2.02% from the MB14 tracks in the case of MB1 failure and HO recovery is estimated to be 3.80%, that is 53% out of the 2.02%. These results are shown in the next table.

MB station	% of muon events	% of HO recovery	relative %
MB12	9.40	8.20	87
MB13	2.18	1.38	63
MB14	3.80	2.02	53

Table 1: Recovery of the HO for a possible failure of the MB1

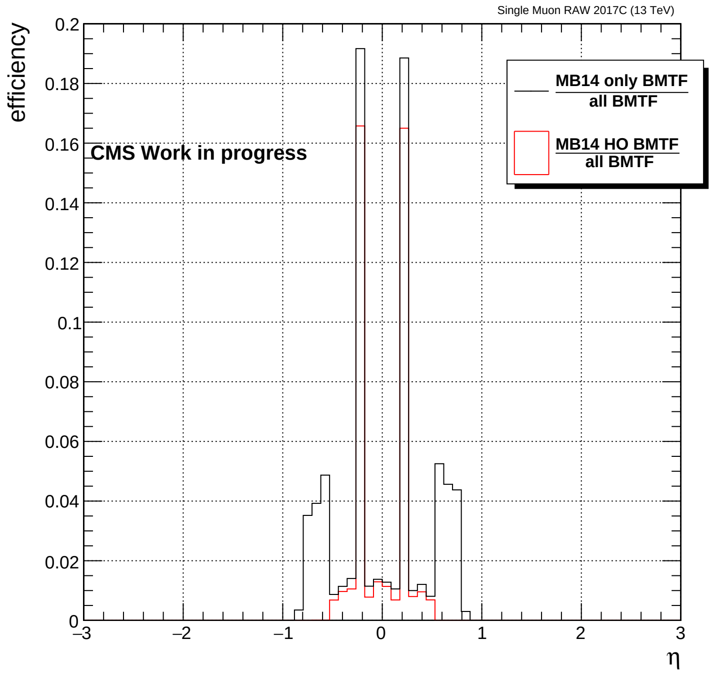

Figure 9: Efficiency of MB14 and HO-MB4

To verify that the results are relevant and significant, the η variable was plotted for every station combinations and compared to that of the corresponding matching with the HO. These results, presented in figures **??**, **??** and **??**, are consistent with the amount of tracks recovered by the HO in each case.

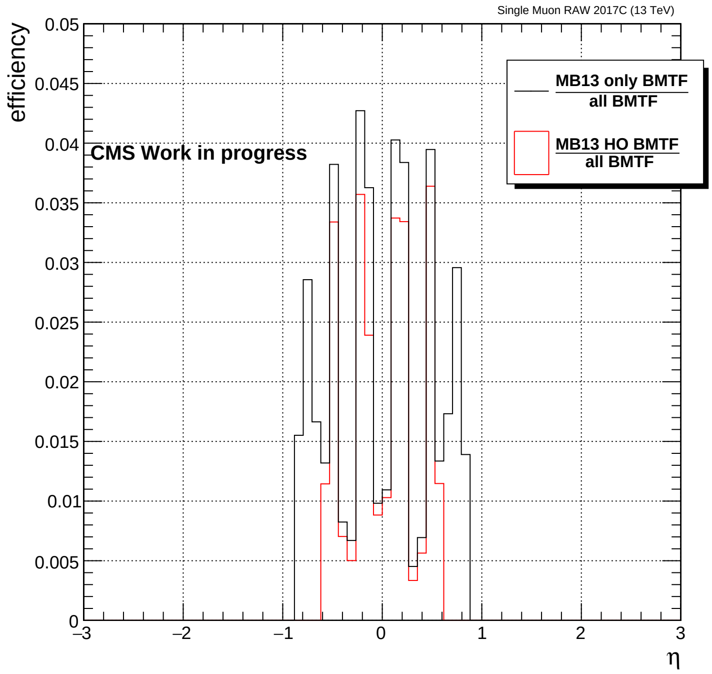

Figure 10: Efficiency of MB13 and HO-MB3

Each figure shows that the HO can recover all over the BMTF coverage region, and this can be concluded from the overlap of the regions against each other.

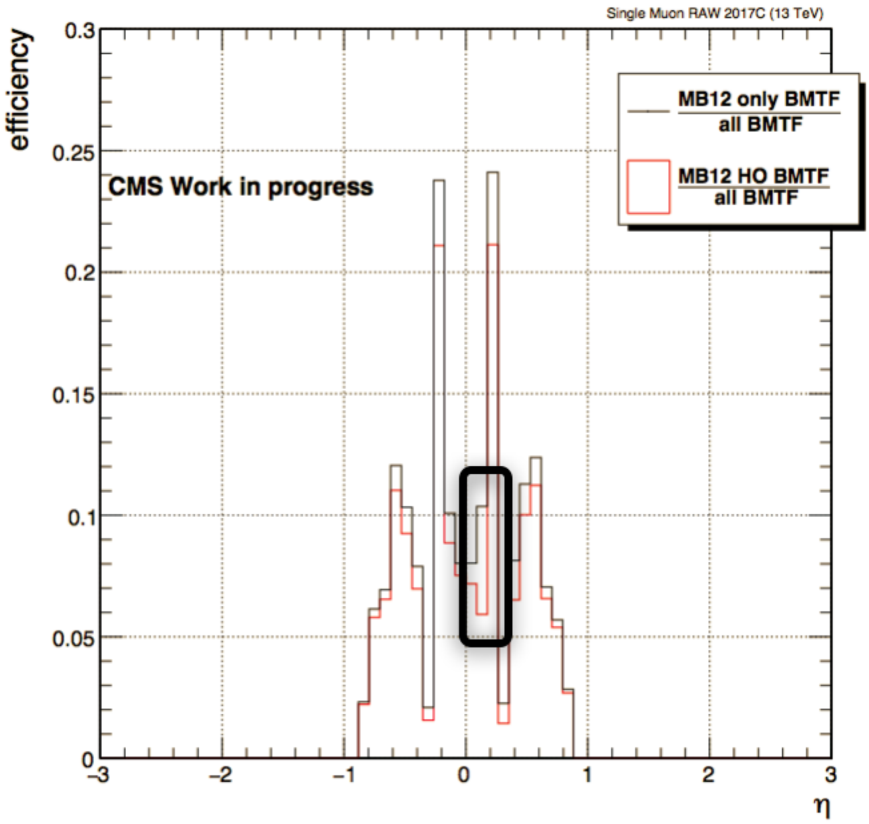

Figure 11: Efficiency of MB12 and HO-MB2. Black square: inefficiency on the HO-MB2, $i\eta = 2$

Nevertheless, there is a small region in the HO-MB2 efficiency that shows an asymmetry between the $i\eta = -2$ and $i\eta = 2$, where the last one presents a lower efficiency as the figure **??** illustrates. Given the geometry of the detector, a symmetrical distribution was expected. Due to this, a more deep analysis has been done.

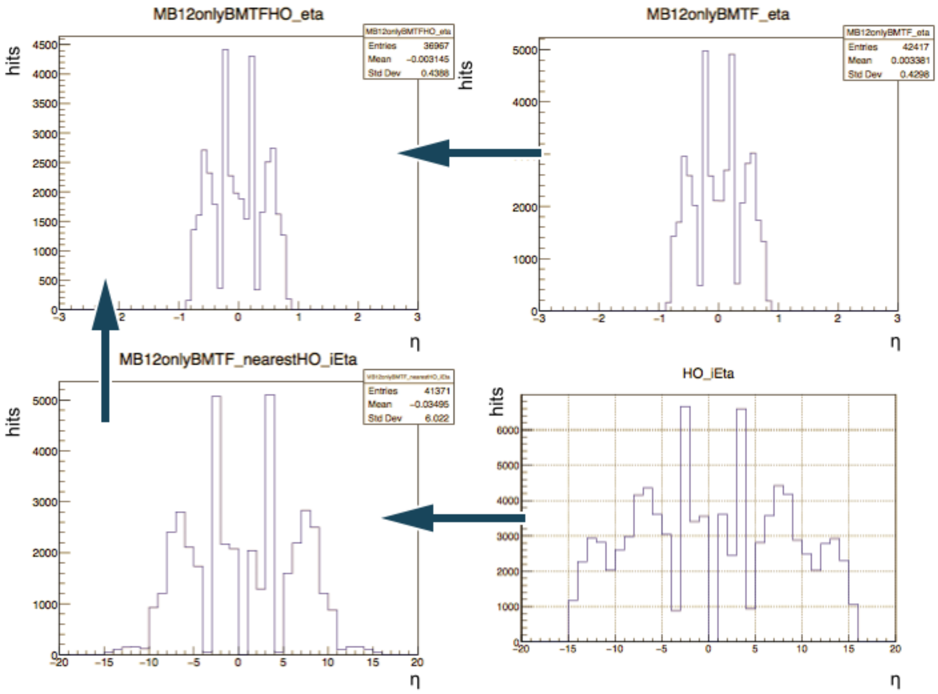

Figure 12: Steps between the MB12 and HO matching

To find the root of this asymmetry, the histograms in figure **??** visualize the $i\eta$ distribution at each step in between in the matching algorithm. From figure **??**, it can be concluded that the problem of this asymmetry is not related to the matching algorithm due that the same inefficiency can be seen even before the matching is done, but that it is directly related to the HO.

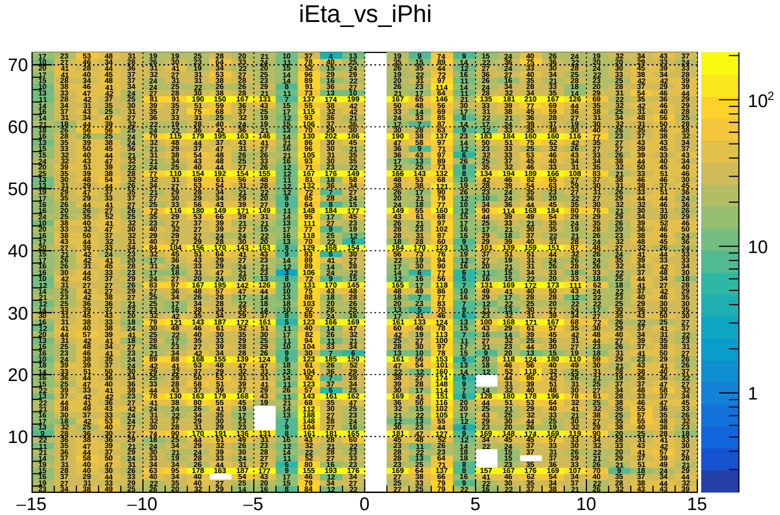

Figure 13: $i\eta$ vs $i\phi$ distribution of the HO

This problem leads to another analysis of the HO to see if every cell in the detector is working properly. Figure **??** shows the distribution of all the entries as a function of $i\eta$ vs $i\phi$ hit count on the HO, where clearly every cell in the $i\eta = 2$ is active and counting. This means the asymmetry doesn't come from a faulty cell nor any other apparent malfunction of the HO. It would be recommended to analyze this behavior to know the root of the asymmetry of detected hits on the HO.

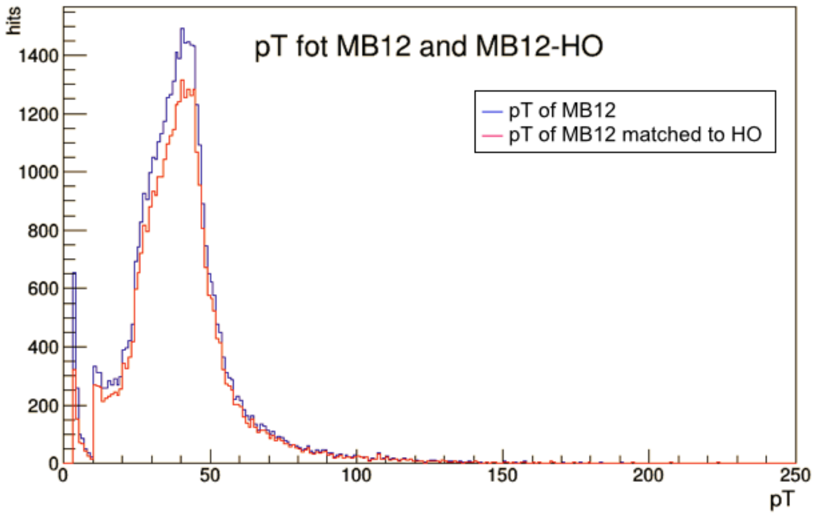

Figure 14: Comparison for the pT

Finally, to compare the tracks formed by the MB12 and the HO-MB2, figure **??** compares the transverse momentum (pT) calculated from the bending angle between them. It is clear from this figure, that for those tracks that are matched, the value of their pT is very similar, because the MB2 station is very close to the HO, therefore the bending angle doesn't have enough space to get further away from the initial detection. On the other hand, for the MB3 and MB4 station the pT assignment is expected to vary due to the size of the HO tiles and the distance between the HO and the MB3 and MB4 respectively.

4 Conclusions

It was determined that the majority of the tracks that are formed from two muon stations come from the MB12 detection, and in case of any failure of the MB1 station, there will be losses of 9.40% from which the HO can recover 87% if it is used as a support system for the muon system. On a similar way, for the MB13 station the HO can recover 63% of lost events out of 2.18% that are lost, and 53% recovery for the MB14 station out of 3.80% that are lost. That supposes a total recovery of 75% of the total lost events in case that the MB1 has to be switch off.
On the other hand, it was found that the HO presents an asymmetry on the count of hits. This study wasn't able to determine the cause of this difference but it gives an insight that there is something that can be analyzed on detail to determine any fail on the detector, if it is the case.

Finally, this study can be extended to include the resolution of the pT estimate for the MB13 and MB14 in case of the HO vain used instead of the MB1.

References

[1] Cooper, S. I. (2016). Phase I Upgrade of the CMS Hadron Calorimeter. Nuclear and Particle Physics Proceedings, 273275, 10021007. https://doi.org/10.1016/j.nuclphysbps.2015.09.157

[2] Scheuch, F. (2017). Studien zu szintillatorbasierten Myontriggern in CMS. RWTH Aachen University, Diss., 2017; 182 Seiten(2017). RWTH Aachen University. https://doi.org/10.18154/rwth-2017-03100

[3] Caminada, L. M., Pauss, F. Study of the Inclusive Beauty Production at CMS and Construction and Commissioning of the CMS Pixel Barrel Detector. Zurich, ETH. CERN-THESIS-2010-149, CMS-TS-2010-026.

[4] Anderson, J., Freeman, J., Los, S., & Whitmore, J. (2012). Upgrade of the CMS Hadron Outer Calorimeter with SIPMs. Physics Procedia, 37, 7278. https://doi.org/10.1016/j.phpro.2012.02.358

[5] Conseil Européen pour la Recherche Nucléaire. About CERN: CMS *https://home.cern/about/experiments/cms*

[6] Bruning, Oliver S. et al. LHC Design Report Vol.1: The LHC Main Ring. CERN-2004-003-V1, CERN-2004-003, CERN-2004-003-V-1

[7] Design, performance, and calibration of CMS hadronbarrel calorimeter wedges, Eur.Phys.J. C55 (2008) 159171. doi:10.1140/epjc/s10052-008-0573-y.

[8] Design, performance, and calibration of the CMS Hadronoutercalorimeter, Eur.Phys.J. C57 (2008) 653663. doi:10.1140/epjc/s10052-008-0756-6.

[9] J. Mans, J. Anderson, B. Dahmes, P. de Barbaro, J. Freeman, T. Grassi, E. Hazen, J. Mans, R. Ruchti, I. Schmidt, T. Shaw, C. Tully, J. Whitmore, T. Yetkin, CMS Technical Design Report for the Phase 1 Upgrade of the Hadron Calorimeter, Tech. Rep. CERN-LHCC-2012-015. CMS-TDR-10, CERN, Geneva, additional contact persons: Jeffrey Spalding, Fermilab, spalding@cern.ch, Didier Contardo, Universite Claude Bernard-Lyon I, contardo@cern.ch (Sep 2012).

[10] Collaboration, T. C., Chatrchyan, S., Hmayakyan, G., Khachatryan, V., Sirunyan, A. M., Adam, W., Riboni, P. (2008). The CMS experiment at the CERN LHC. Journal of Instrumentation, 3(8), S08004S08004. https://doi.org/10.1088/1748-0221/3/08/s08004